**Numerical simulation on the influence of metal radiation shield on the thermal insulation performance of the semi-transparent materials**

***Fengfei LOU[a], Sujun DONG[a], Xiaona CHEN[b], Jiangfeng GUO[b], Keyong ZHU[a*]***

[a] School of Aeronautic Science and Engineering, Beihang University, Beijing 100191, PR China

[b] Beijing Aerospace Technology Institute, Beijing 100074, PR China

*Corresponding author: Keyong ZHU; E-mail: zhukeyong@buaa.edu.cn

*Foams, flexible felt and thermal barrier coatings are widely used in the thermal insulation fields. This type of material has lower density and thermal conductivity, as well as higher specific surface area and porosity, and is generally referred to as the semi-transparent materials. The radiation heat transfer inside the semi-transparent materials belongs to medium radiation, so the radiation thermal conductivity is larger at high temperature. However, the metal radiation shields (MRSs) play an important role in weakening radiation heat transfer. In order to study the effect of MRSs on the thermal insulation performance of the semi-transparent materials, the numerical simulation of coupling heat transfer of heat conduction and heat radiation is carried out. The effective thermal conductivity (ETC) of the semi-transparent materials with different extinction coefficient is calculated when the different layers of MRSs are evenly inserted into the semi-transparent materials at the specific temperature, so that the influence of MRSs on the thermal insulation performance of the semi-transparent materials can be obtained. The simulation results show that whether it is an optical thin medium or an optical thick medium, when 7 layers of MRSs are inserted into the semi-transparent materials, the thermal insulation performance is greatly improved. After that, the ETC changes little with the increase of the layer of MRSs.*

Keywords: *semi-transparent materials, effective thermal conductivity, metal radiation shield, numerical simulation*

## 1 Introduction

Whether in the construction or industrial fields, high temperatures can cause equipment damage [1]. Thermal insulation materials play a very important role in this respect. Foams, flexible felt and thermal barrier coating are widely used in the thermal insulation fields [2-5]. This type of material has lower density and thermal conductivity, as well as higher specific surface area and porosity, and is generally referred to as the semi-transparent materials [6-7].

The semi-transparent materials are participatory medium for radiation heat, and the radiation heat transfer inside the materials belongs to medium radiation [8-9]. They have strong permeability to near-infrared radiation with wavelength of 3~8 μm at high temperature, which leads to poor infrared radiation shielding ability at high temperature, and the radiation thermal conductivity increases significantly with the increase of temperature, thus limiting the application of the semi-transparent materials in the thermal insulation field [10-12].

In view of this shortcoming, most of the researches focus on the use of opacifier with absorption and scattering effects on near-infrared radiation [13]. By using opacifier, the thermal radiation inside the semi-transparent materials will be simultaneously absorbed and scattered. The ability to suppress radiation heat in materials can be characterized by extinction coefficient (extinction coefficient $\beta$ = absorption coefficient $\kappa$ + scattering coefficient $\sigma$), which is an indicator for evaluating the overall absorption and scattering effects. However, for opacifier particles that inhibit radiation heat, diameters of opacifier particles are all in the order of microns. The addition of micron-sized functional additives will enhance the heat transfer of the semi-transparent materials because of high thermal conductivity of opacifier [14-16].

However, because the metal radiation shields (MRSs) play an important role in weakening radiation heat transfer, it is widely used in engineering technology [17-18]. In the steam turbine, in order to reduce the radiation heat transfer between the inner and outer sleeves, a cylindrical metal radiation shield made of stainless steel is installed between them to reduce the radiation heat transfer between the inner and outer sleeves [19].

The above researches only focus on the application of MRSs in engineering technology, but no scholars have ever studied the influence of MRSs on the thermal insulation performance of the semi-transparent materials with different extinction coefficient. In this paper, firstly, the effective thermal conductivity (ETC) of the semi-transparent materials with different extinction coefficient at different hot surface temperatures is calculated without any MRS. Secondly, the ETC of the semi-transparent materials with different extinction coefficient at specific hot surface temperature is calculated when different layers of MRSs are inserted into semi-transparent materials. Thirdly, the ETC of the semi-transparent materials is calculated at different hot surface temperatures without MRS and with 7 layers of MRSs.

## 2 Methodology and model introduction

### 2.1 Methodology

In order to study the influence of MRSs on the thermal insulation performance of the semi-transparent materials, the following three calculation steps are carried out respectively. Firstly, the numerical simulation of coupling heat transfer of heat conduction and heat radiation is carried out to calculate the ETC of the semi-transparent materials with different extinction coefficient at different hot surface temperatures, so as to obtain the ETC of different diathermic media at different temperatures. Secondly, in order to reduce the ETC, at the specific hot surface temperature, the ETC of the semi-transparent materials with different extinction coefficient is calculated when different layers of MRSs are inserted into semi-transparent materials. Thirdly, under the specific extinction coefficient, the simulation calculation is carried out at different hot surface temperatures. By calculating the ETC of the semi-transparent materials without any MRS and with 7 layers of MRSs, the reduction percentage of ETC of the semi-transparent materials with 7 layers of MRSs is quantitatively analyzed.

Firstly, the computational domain of the semi-transparent materials without any MRS is shown in Fig. 1, and the computational domain is a three-dimensional structure. The length, width and height are 200 mm, 200 mm and 10 mm respectively. The side edges are in adiabatic state, and the bottom and top surfaces are set as isothermal boundaries, that is, the cold surface temperature $T_C$ and the hot surface temperature $T_H$ respectively. The $T_C$, $T_H$, absorption coefficient $\kappa$ and scattering coefficient $\sigma$ are shown in Fig. 2 respectively.

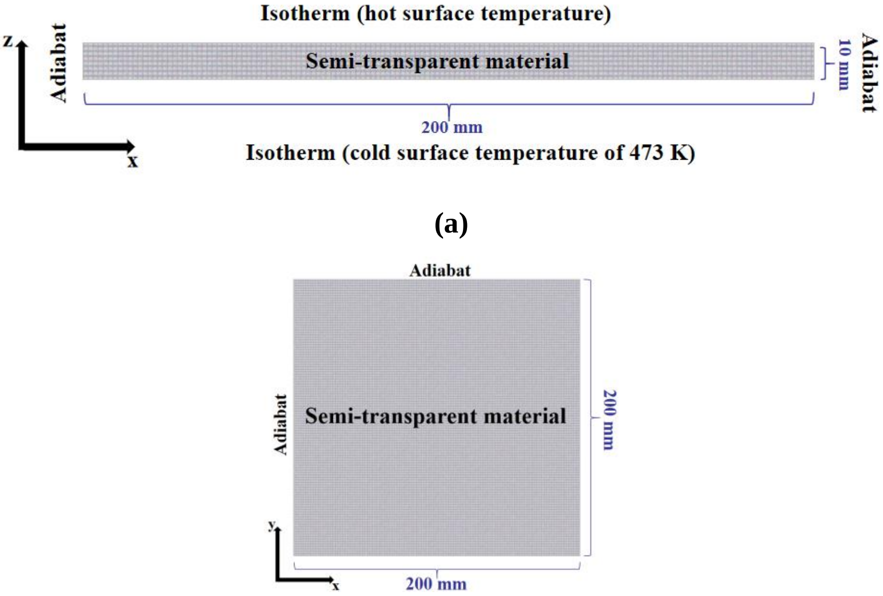


**Fig. 1 The computational domain: (a) Front view; (b) Top view.**

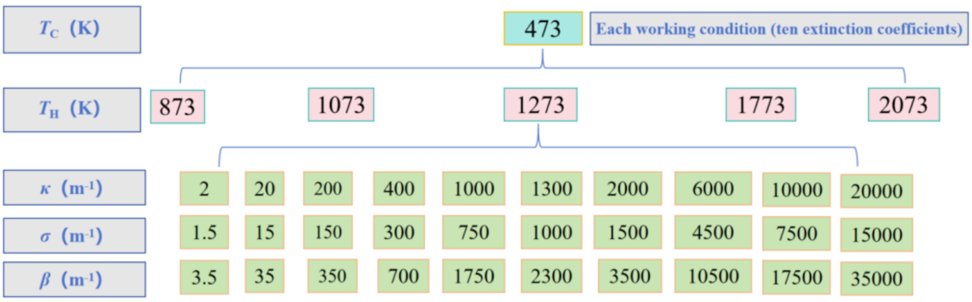


**Fig. 2 Calculation condition of the computational domain without MRS.**

Based on the above questions, one-dimensional Fourier steady-state thermal conductivity calculation method is used to calculate the thermal conductivity of the semi-transparent materials, which is called ETC [20, 21]. The energy equation of coupling heat transfer of heat conduction and heat radiation and Radiative Transfer Equation (RTE) are solved by Finite Volume Method (FVM) and Discrete Ordinates Method (DOM) respectively [22, 23]. Given the $\kappa$, $\sigma$, $T_H$ (boundary temperature) and $T_C$ of 473 K, ETC can be calculated by Eq. (1).

$$\lambda_{\text{eff}} = q_t \delta / \Delta T \tag{1}$$

where $q_t$ and $\Delta T$ are the total heat flux and temperature difference across the semi-transparent materials, $\delta$ is the overall thickness of the semi-transparent materials. The ETC obtained from one-dimensional Fourier steady-state calculation method is regarded as the true thermal conductivity of the semi-transparent materials [20, 21].

Secondly, the ETC of the semi-transparent materials with different layers of MRSs is calculated. The $T_C$, $T_H$, $\kappa$, $\sigma$ and number $N$ of inserted MRSs are shown in Fig. 3 respectively. It should be pointed out here that the overall thickness of the semi-transparent materials is 10 mm, and the thickness of one layer of MRS is 0.01 mm. During the simulation process, the multi-layer MRSs are uniformly inserted into the semi-transparent materials, as shown in Fig. 4, which is a schematic diagram when one layer of MRS and four layers of MRSs are inserted into the semi-transparent materials respectively.

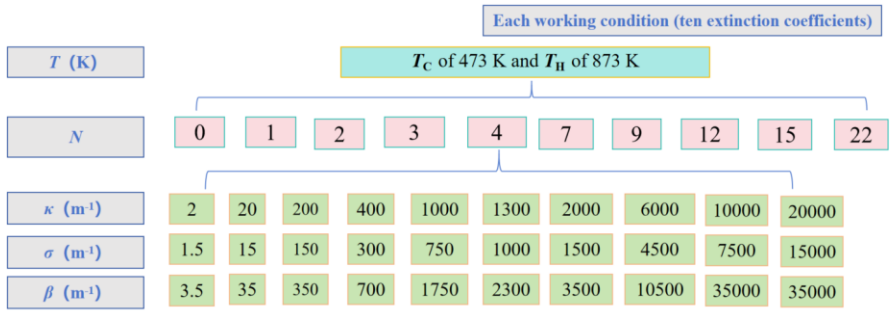


**Fig. 3 Calculation condition of the computational domain with MRSs.**

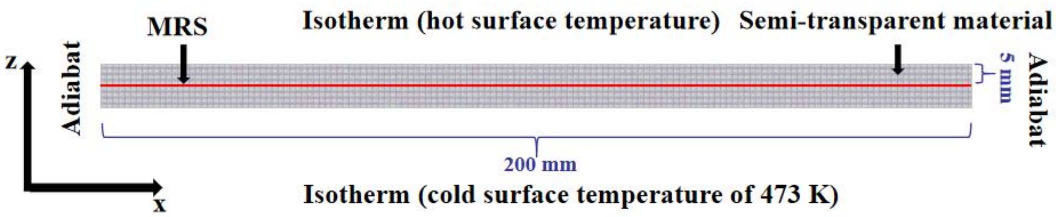


**(a)**

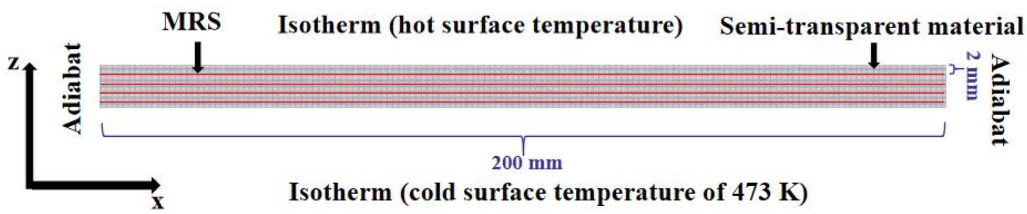


**(b)**

**Fig. 4 Number *N* of layers of MRSs: (a) One layer of MRS; (b) Four layers of MRSs.**

Thirdly, when the $\kappa$ and $\sigma$ are constant, the ETC of the semi-transparent materials without any MRS and with 7 layers of MRSs at different $T_H$ are calculated respectively, so that the influence of MRSs on the thermal insulation performance of the semi-transparent materials is quantitatively analyzed. The $T_C$, $T_H$, $\kappa$, $\sigma$ and $N$ are shown in Fig. 5 respectively.

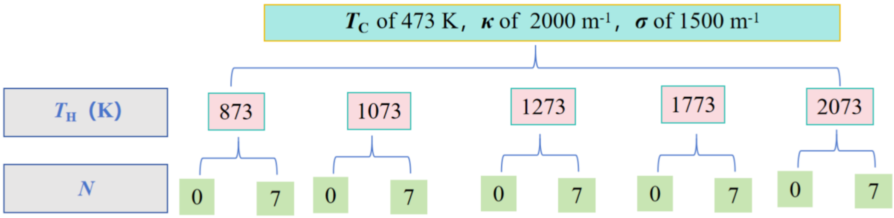


**Fig. 5 Calculation condition of the computational domain with 7 layers of MRSs.**

## 2.2 Model introduction

### *2.2.1 Computational domain and boundary conditions*

The boundary conditions are adiabatic on the sides, and the cold and hot surfaces are isothermal boundaries. The $T_C$ is set to 473 K, the $T_H$ are set to 5 different values, and the $\kappa$ and $\sigma$ are set to 10 different values respectively. The internal emissivity of the semi-transparent materials is 0.85 for all cases, and the internal emissivity of MRS is 0.05. The thermophysical properties of MRS and semi-transparent materials are shown in Tab. 1.

**Tab. 1 The thermophysical properties.**

| Parameter / Material | density $\rho$ (kg/m$^3$) | Specific heat capacity $c$ (J/ (kg K)) | Thermal conductivity $\lambda$ (W/ (m K)) |
|---|---|---|---|
| MRS | 2719 | 871 | 202.4 |
| Semi-transparent material | 200 | 1000 | 0.02 |

### *2.2.2 Grid independence verification*

For the verification of grid independence, when no MRS is inserted into the semi-transparent materials, the $\kappa$ and $\sigma$ are set to 2000 m$^{-1}$ and 1500 m$^{-1}$ respectively, the $T_H$ and $T_C$ are set to 873 K and 473 K respectively, and the side is in adiabatic state, so as to calculate ETC. The Fig. 6 shows the change of the ETC with the number of grids, from which that when the number of grids reaches 857,613, the ETC no longer changes with the increase of the number of grids. In the actual calculation process, the number of grids of 1,101,973 is finally selected to calculate the ETC.

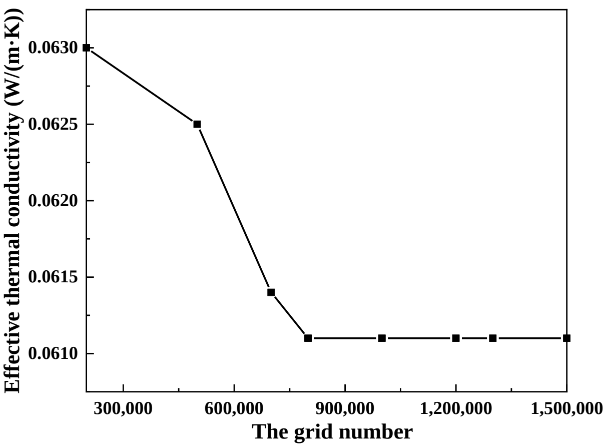


**Fig. 6 The variation of ETC with the number of grids.**

## 3 Numerical method

### 3.1 Numerical method

#### *3.1.1 Governing equations*

Taking the computational domain of the semi-transparent materials as an example, the energy equation within the semi-transparent materials is:

$$\rho c \frac{\partial T}{\partial t} = -\nabla \cdot \boldsymbol{q}_{\mathrm{t}} = -\nabla \cdot \boldsymbol{q}_{\mathrm{c}} - \nabla \cdot \boldsymbol{q}_{\mathrm{r}} = \frac{\partial}{\partial x}\left(\lambda \frac{\partial T}{\partial x}\right) + \frac{\partial}{\partial y}\left(\lambda \frac{\partial T}{\partial y}\right) + \frac{\partial}{\partial z}\left(\lambda \frac{\partial T}{\partial z}\right) - \nabla \cdot \boldsymbol{q}_{\mathrm{r}} \tag{2}$$

where $\boldsymbol{q}_{\mathrm{t}}$, $\boldsymbol{q}_{\mathrm{c}}$, $\boldsymbol{q}_{\mathrm{r}}$ are total heat flux, conductive heat flux and radiation heat flux. The radiation heat flux is related to the radiative intensity within the materials, and the specific calculation equations are shown below:

$$\boldsymbol{q}_{\mathrm{r}} = q_{r,x}\boldsymbol{e}_x + q_{r,y}\boldsymbol{e}_y + q_{r,z}\boldsymbol{e}_{\mathrm{z}} \tag{3}$$

$$q_{r,x} = \int_{\Omega=4\pi} I\xi \mathrm{d}\Omega \tag{4}$$

$$q_{r,y} = \int_{\Omega=4\pi} I\eta \mathrm{d}\Omega \tag{5}$$

$$q_{r,z} = \int_{\Omega=4\pi} I\mu \mathrm{d}\Omega \tag{6}$$

where $q_{r,x}$ ($\xi$=sin$\theta$cos$\varphi$), $q_{r,y}$ ($\eta$=sin$\theta$sin$\varphi$) and $q_{r,z}$ ($\mu$=cos$\theta$) are the components of radiation heat flux in *x*, *y* and *z* coordinates respectively; $\xi$ is direction cosine along the *x* coordinate axis, $\eta$ is direction cosine along the *y* coordinate axis and $\mu$ is direction cosine along the *z* coordinate axis respectively; $\theta$ and $\varphi$ are zenith angle and azimuthal angle respectively; $\Omega$ is solid angle; $I$ is radiative intensity.

Among them, $\boldsymbol{q}_{\mathrm{t}}$, $\boldsymbol{q}_{\mathrm{c}}$ and $\boldsymbol{q}_{\mathrm{r}}$ in Eq. (2) and Eq. (3) are all vectors, which can be divided into components along *x* coordinate axis, *y* coordinate axis and *z* coordinate axis according to the heat transfer model. The Eqs. (4), (5) and (6) represent the components of radiation heat flux in *x*, *y* and *z* coordinates respectively, where the radiative intensity needs to be solved.

The radiative intensity within the semi-transparent materials is governed by RTE, and the RTE is shown in Eq. (7). The boundary wall of opaque, diffuse emission and diffuse reflection is used in this calculation model, so the corresponding boundary condition is shown in Eq. (8).

$$\frac{\mathrm{d}I(r,\boldsymbol{s})}{\mathrm{d}r} = -\beta I(r,\boldsymbol{s}) + \kappa I_{\mathrm{b}}(r) + \frac{\sigma}{4\pi}\int_{\Omega_{\mathrm{i}}=4\pi} I(r,\boldsymbol{s}_{\mathrm{i}})\Phi(\boldsymbol{s}_{\mathrm{i}},\boldsymbol{s})\mathrm{d}\Omega_{\mathrm{i}} \tag{7}$$

$$I_w(\boldsymbol{s}) = \varepsilon_w I_{\mathrm{b},w} + \frac{1-\varepsilon_w}{\pi}\int_{n_w\cdot s_{\mathrm{i}}<0} I_w(\boldsymbol{s}_i)\left|\boldsymbol{n}_w \cdot \boldsymbol{s}_{\mathrm{i}}\right| \mathrm{d}\Omega_{\mathrm{i}} \tag{8}$$

where $I_{\mathrm{b}}(r)$ is radiative intensity emitted by a black body; $I(r,\boldsymbol{s})$ represents the incident radiative intensity of space position *r* and transmission direction $\boldsymbol{s}$; $\Phi(\boldsymbol{s}_{\mathrm{i}},\boldsymbol{s})$ is scattering phase function, which is the ratio of the scattering intensity in the ***s*** direction caused by incident radiation in the $\boldsymbol{s}_{\mathrm{i}}$ direction to the average scattering intensity in the 4π scattering space. Here, because RTE is related to space and direction, $I(r,\boldsymbol{s})$, $I(r,\boldsymbol{s}_i)$ and $\Phi(\boldsymbol{s}_i,\boldsymbol{s})$ in the Eq. (7) are all related to direction, which are vectors. $I_w$ is the radiation intensity of the wall; $\varepsilon_w$ is emissivity of wall; $T_w$ is temperature of wall; $\boldsymbol{n}_w$ is the normal vector of wall.

### *3.1.2 Numerical methods*

It is necessary to know the radiative intensity to solve the heat flux filed within the semi-transparent materials in Eq. (2) which is relying on solving Eqs. (7) and (8). Meanwhile, the heat flux field should be known to determine the radiative intensity field in Eq. (7). Therefore, Eqs. (2) and (7) should be solved alternately until consistency is reached between heat flux filed and radiative intensity field at each time step. The energy equation and RTE are solved by FVM and DOM respectively.

In the DOM, radiation intensity needs to be discretized in direction and space. For the calculation model, under the condition of three-dimensional space coordinate system (*x*, *y*, *z*), the RTE on the discrete direction ($\xi^m$, $\eta^m$, $\mu^m$) is shown in Eq. (9). The boundary wall of opaque, diffuse emission and diffuse reflection is used in this calculation model, so the corresponding boundary condition is shown in Eq. (10). Finally, the discrete formula in each direction is discretized again in space by finite difference method, thus the radiation intensity is obtained.

$$\xi^m \frac{\partial I^m}{\partial x} + \eta^m \frac{\partial I^m}{\partial y} + \mu^m \frac{\partial I^m}{\partial z} = -\beta I^m + \kappa I_b(r) + \frac{\sigma}{4\pi}\left[\sum_{l=1}^{N\Omega} w^l I^l \Phi^{m,l}\right] \tag{9}$$

$$I_w^m = \varepsilon_w I_{b,w} + \frac{1-\varepsilon_w}{\pi} \sum_{\boldsymbol{n}_w \cdot \boldsymbol{s}_l < 0} w^l I_w^l \left|\boldsymbol{n}_w \cdot \boldsymbol{s}_l\right|, \quad \boldsymbol{n}_w \cdot \boldsymbol{s}_m > 0 \tag{10}$$

where $l$ and $m$ represent the $l_{\text{th}}$ and $m_{\text{th}}$ solid angle of space direction respectively; $N\Omega$ is the total number of solid angles with space direction of 4π; $w^l$ is the integral weight coefficient; $\Phi^{m,l}$ is the scattering phase function after discretization.

In this paper, the numerical simulation of Computational Fluid Dynamics is performed to solve the governing equations. The commercial software ICEM is used to generate the mesh, and Eqs. (2)-(8) are solved by commercial software Fluent 2022 R1. Both the energy equation and RTE are discretized using second order upwind scheme while the unsteady item of energy equation is discretized with second order implicit scheme. The iterative process will stop until the residuals of energy equation and RTE is less than 1.0E-10.

## 3.2 Validation of numerical method

The semi-transparent materials are participatory medium of radiation heat, and the radiation heat transfer inside the materials belongs to medium radiation. Lou et al. [24] pointed out that due to the medium radiation of the semi-transparent materials, not only the radiation thermal conductivity of materials at high temperature is larger, but also the test methods of thermal conductivity have a large error.

On the one hand, for the test methods of the thermal conductivity of the semi-transparent materials, Lou et al. [20] and Zhang et al. [21, 22, 23] conducted a series of numerical simulations of the coupling heat transfer of heat conduction and heat radiation for thermal conduction heating method to study the influence of medium radiation on the test results. Dai et al. [25] also carried out numerical simulation of coupling heat transfer for three methods (thermal conduction heating method, convection heating method and radiation heating method). At the same time, Zhang et al. [26] conducted a series of experiments on the test methods, and the test results showed that the temperature rise curve of the semi-transparent materials obtained by the radiation heating method is higher than that of the convection heating method, which is similar to the change trend of the simulation results obtained by Dai et al. [25], thus proving the accuracy of the numerical simulation.

On the other hand, the numerical simulation of the coupling heat transfer of heat conduction and heat radiation of semi-transparent materials with different $\beta$ is performed by using the numerical method of this paper, and the results are compared with those calculated by Zhang et al. [21], as shown in Fig. 7 (the model and calculation conditions are the same). It can be seen from Fig. 7 that the calculated results are the same as those calculated by Zhang et al. [21], so the numerical method in this paper can also be verified.

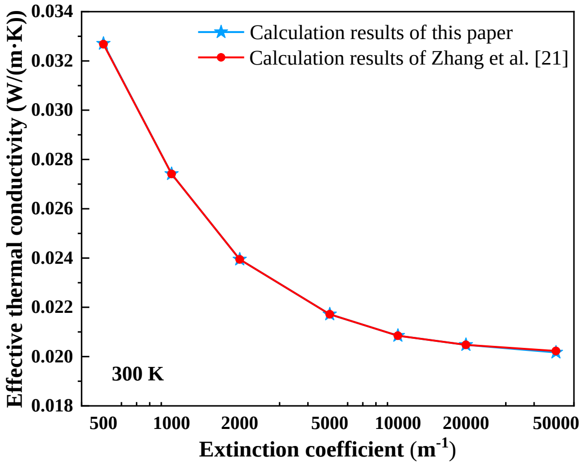


**Fig. 7 Validation of numerical method.**

Based on the above analysis, the numerical method (the energy equation and RTE are solved by FVM and DOM respectively) are widely used in the calculation process of the semi-transparent materials [20, 21, 22, 23, 25]. It can be seen in the references that the variation trend of numerical results is similar to the experimental results [25, 26], and for the same model, the calculation results of this paper are also the same as the simulation results calculated by Zhang et al. [21], which can prove the accuracy of the numerical method. Therefore, when studying the influence of MRSs on the thermal insulation performance of semi-transparent materials, the numerical results obtained by the numerical method used in this paper are reliable.

## 4 Results and discussion

### 4.1 Calculation of ETC

When no MRS is inserted into the semi-transparent materials, the ETC of the semi-transparent materials with different $\beta$ changes with the $T_H$ as shown in Fig 8. In the calculation model, the side surface is set to adiabatic state, the $T_C$ is set to 473 K, and the hot surface is set to various temperatures, thus calculating ETC.

The optical thickness of the semi-transparent materials with different $\beta$ is the product of $\beta$ and characteristic thickness $\delta$ of specimen (optical thickness $\tau = \beta \times \delta$, the characteristic thickness $\delta$ of semi-transparent materials is 0.01 m). Theoretically, when the optical thickness is much greater than 1, the semi-transparent material is called optical thick media, and conversely, they are called optical thin media.

As can be seen from Fig 8(a), whether it is the optical thin medium or the optical thick medium, ETC has an upward trend with temperature in different degrees. When the optical thickness is 0.035, 0.35, 3.5 and 7, ETC increases greatly with temperature. While when the optical thickness is large, ETC changes slightly with temperature compared to optical thin media. As shown in Fig 8(b), when the optical thickness is 0.035, compared to the ETC at 873 K, the increase percentages of ETC at 1073 K, 1273 K, 1773 K and 2073 K are 57.6%, 136%, 449% and 733% respectively. When the optical thickness is 350, compared to the ETC at 873 K, the increase percentages of ETC at 1073 K, 1273 K, 1773 K and 2073 K are 28.1%, 66.5%, 219% and 358% respectively.

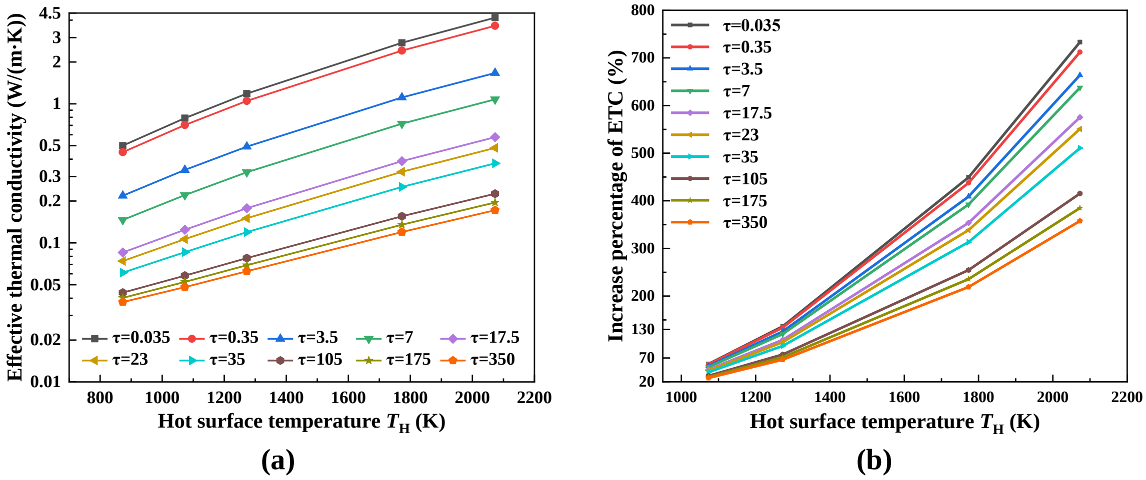


**Fig. 8 The variation of ETC: (a) The variation of ETC at different $T_H$; (b) Increase percentage of ETC at different $T_H$.**

As shown in Fig 9, it is the temperature curve along the *z*-axis direction at the boundary of the semi-transparent materials with different $\beta$. The larger the $\beta$ is, the trend of temperature curve is the same as that of heat conduction.

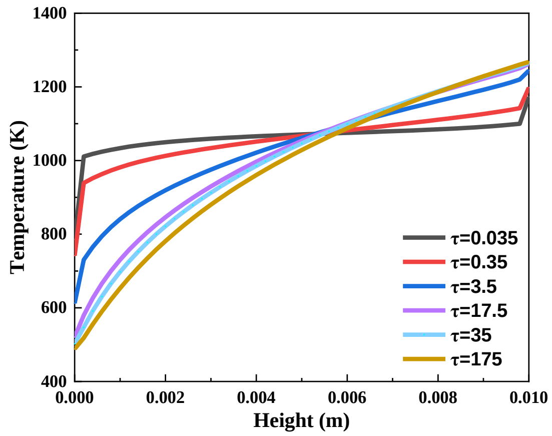


**Fig. 9 Temperature curve along *z*-axis direction at boundary of semi-transparent materials.**

The reason for this phenomenon is that the larger the optical thickness, the stronger the suppression of thermal radiation. When the optical thickness is much greater than 1, the material is called the optical thick medium, which assumes that thermal radiation penetrates only a very short distance. In optical thick materials, the coupling heat transfer process of heat conduction and heat radiation inside the materials can be regarded as a heat diffusion process, so the influence of radiation heat transfer is very small. Therefore, when the optical thickness of the material is large, with the increase of the hot surface temperature, the increase of the ETC is smaller than that of the optical thin medium.

### 4.2 Effect of the MRSs on the thermal insulation performance

Through the steady-state calculation of numerical simulation, the $T_H$ and $T_C$ are set to 873 K and 473 K respectively, and the surrounding area is set as adiabatic state. The different layers $N$ of MRSs are inserted into the semi-transparent materials to calculate ETC. As shown in Fig 10, for media with small optical thickness, that is, optical thin media, as long as the MRS is inserted into the semi-transparent materials, the ETC will decrease, and the ETC will decrease more with the increase of $N$. However, when $N$ are 7 layers, the change of ETC is very small with the increase of $N$.

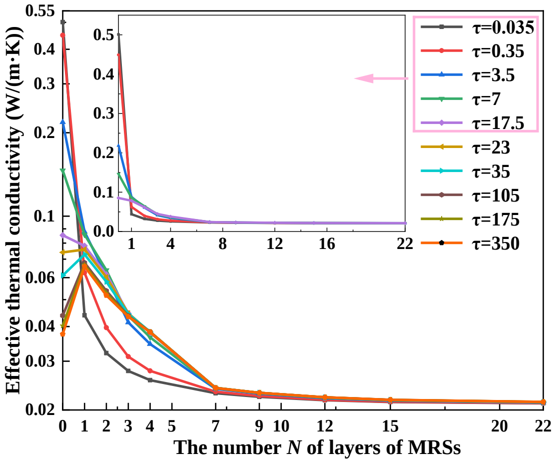


**Fig. 10 The influence of *N* on the thermal insulation performance.**

For optical thin media, the reduction percentage of ETC is shown in Fig 11(a) when the MRSs are inserted into the semi-transparent materials compared to the materials without MRS. When the $\kappa$ and $\sigma$ are 2 $m^{-1}$ and 1.5 $m^{-1}$ respectively, that is, when the optical thickness is 0.035, compared to the materials without MRS, the reduction percentage of ETC of the semi-transparent materials in layers of 1, 2, 3, 4, 7, 9, 12, 15 and 22 inserted are 91.2%, 93.6%, 94.4%, 94.8%, 95.4%, 95.5%, 95.6%, 95.7% and 95.8% respectively.

For optical thick media, when no MRS is inserted into the semi-transparent materials, the ETC is much smaller than that of optical thin media. As shown in Fig 10, the thermal insulation performance of the semi-transparent materials is not improved when fewer MRSs are inserted into semi-transparent materials with larger optical thickness. However, when the $N$ are 7 layers, the thermal insulation performance is greatly improved, and then the ETC is basically unchanged with the increase of $N$. As shown in Fig 11(b), when the optical thicknesses are 0.035, 0.35, 3.5, 7, 17.5, 23, 35, 105, 175 and 350 respectively, the ETC decreases by 95.4%, 94.8%, 89.1%, 83.6%, 71.9%, 67.5%, 60.7%, 45.2%, 40% and 36.1% respectively when the 7 layers of MRSs are inserted into semi-transparent materials compared to the semi-transparent materials without MRS.

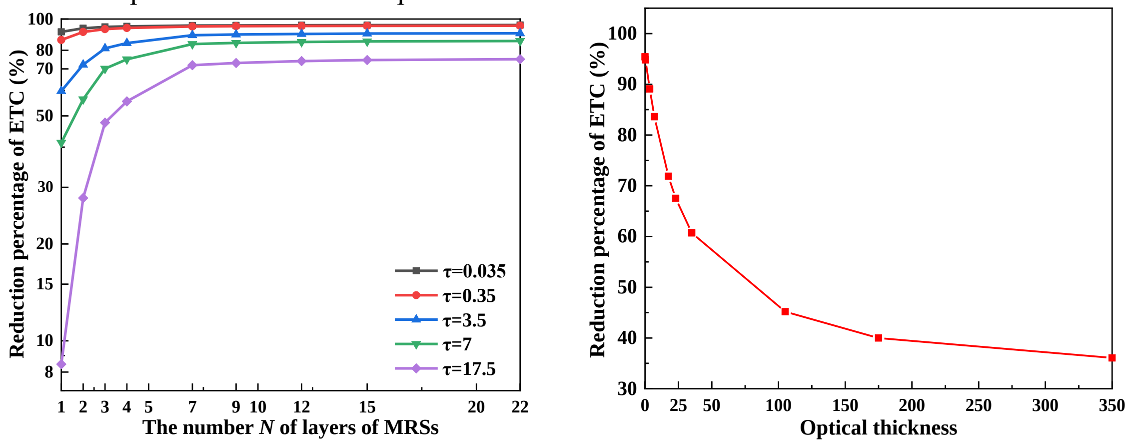


**(a) (b)**

**Fig. 11. Reduction percentage of ETC: (a) different *N* compared to no MRS; (b) 7 layers of MRSs compared to no MRS.**

When the $\kappa$ and $\sigma$ are 20 and 15 respectively, that is, the optical thickness is 0.35, when different layers of MRSs are inserted into the semi-transparent materials, the temperature at center of semi-transparent material changes with the *z*-axis direction as shown in Fig 12. When the *N* are large, the temperature curve of the center position of the semi-transparent materials along the *z*-axis direction tends to be the temperature curve during heat conduction.

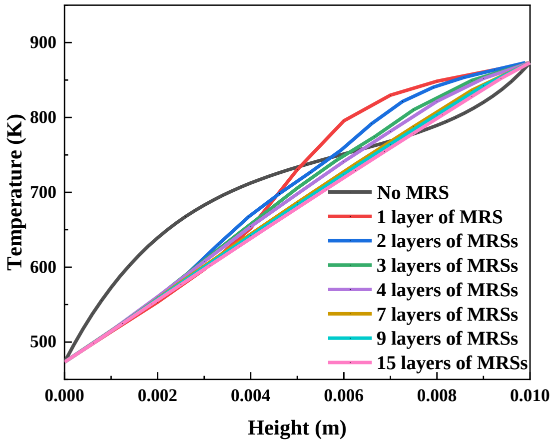


**Fig. 12 Temperature curve along *z*-axis direction at center of semi-transparent material.**

For optical thick media, because the heat radiation penetrates only a short distance, the coupling heat transfer process of heat conduction and heat radiation inside the materials can be regarded as a diffusion process, and the influence of radiation heat is very small. However, for optical thin media, the radiation penetration distance is longer, so the radiation heat has a greater impact. The function of the MRS is to weaken the radiation heat transfer, so the effect of reducing the radiation heat transfer is more effective when the MRS is inserted in the optical thin medium than the optical thick medium.

For the semi-transparent materials with small extinction coefficient, when more MRSs are inserted into the semi-transparent materials, the radiation heat transfer can be greatly reduced, so the temperature distribution of semi-transparent materials along the *z*-axis direction is a straight line with constant slope, which is similar to the temperature distribution calculated when there is only heat conduction.

### 4.3 Quantitative analysis of the influence of *N*

The semi-transparent materials are generally the optical thick medium. In order to quantitatively analyze the effect of MRS on thermal insulation performance of the semi-transparent materials, the numerical simulation of coupling heat transfer of heat conduction and heat radiation is performed. When the $\kappa$ and $\sigma$ are set to 2000 $m^{-1}$ and 1500 $m^{-1}$ respectively, the $T_C$ is set to 473 K, the surrounding area is set to adiabatic state, and the $T_H$ are set to 873 K, 1073 K, 1273 K,1773 K and 2073 K respectively, the ETC of the semi-transparent materials without any MRS and with 7 layers of MRSs are calculated respectively.

As shown in Fig. 13, when the $T_H$ are 873 K, 1073 K, 1273 K, 1773 K and 2073 K respectively, the reduction percentage of ETC is 60.7%, 70%, 76.6%, 85.6% and 88.1% respectively when 7 layers of MRSs are inserted into the materials. With the increase of temperature, the reduction percentage of ETC is greater, mainly because the higher the temperature, the greater the proportion of radiation thermal conductivity. The MRS is mainly used to reduce radiation heat transfer, so the reduction percentage of ETC is greater.

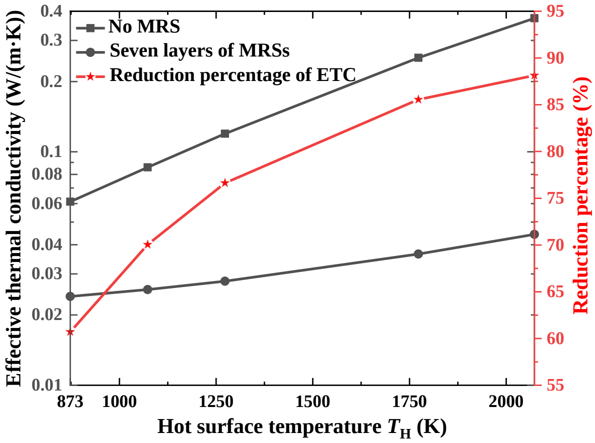


**Fig. 13 Reduction percentage of ETC of materials with 7 layers of MRSs at different $T_H$**

## 5 Conclusions

In this paper, the numerical simulation of coupling heat transfer of heat conduction and heat radiation is carried out to study the influence of MRS on the thermal insulation performance of the semi-transparent materials.

Whether it is an optical thin medium or an optical thick medium, the numerical simulation results show that when 7 layers of MRSs are inserted into the semi-transparent materials, the thermal insulation performance of the semi-transparent materials is greatly improved, and then the ETC changes very little with the increase of the number of layers of MRSs. When the cold surface temperature and the hot surface temperature are 473 K and 873 K respectively, the optical thicknesses are 0.035, 0.35, 3.5, 7, 17.5, 23, 35, 105, 175 and 350 respectively, the ETC decreases by 95.4%, 94.8%, 89.1%, 83.6%, 71.9%, 67.5%, 60.7%, 45.2%, 40% and 36.1% when the 7 layers of MRSs are inserted into the materials respectively.

## Acknowledgment

This work was supported by the National Natural Science Foundation of China (Grant No. 11902026 & 52206001)

## Reference

[1] Lou, F., *et al.*, Structure Design and Performance Test of a High Temperature Rise Combustor based on Combustion-Gas Wind Tunnel Device, *Heat Transfer Research*, *53*(2022), pp. 21–36.

[2] Ivanov, V. S., *et al.*, Hydrogen Fueled Detonation Ramjet: Conceptual Design and Test Fires at Mach 1.5 and 2.0, *Aerospace Science and Technology*, *109* (2021), pp. 1–12.

[3] Lou, F., *et al.*, Thermal Conductivity Test and Model Modification of $SiO_2$ Aerogel Composites based on Heat Flow Meter Method, *Applied Thermal Engineering*, *254*(2024), pp. 123877.

[4] Li, C.; *et al.*, A Review of Silicon-based Semi-transparent Materials Thermal Insulation Materials: Performance Optimization through Composition and Microstructure, *Journal of Non-Crystalline Solids*, *553*(2021), pp. 120517.

[5] Elshazli, M., *et al.*, Experimental Study of Using Semi-transparent Materials Insulation for Residential Buildings, *Advances in Building Energy Research*, *16*(2022), pp. 569-588.

[6] Merillas, B., *et al.*, Thermal Conductivity of Nanoporous Materials: Where Is the Limit? *Polymers*, *14*(2022), pp. 2556.

[7] Liu, H., *et al.*, Geometric Optimization of Semi-Transparent Materials Composites for High Temperature Thermal Insulation Applications, *Journal of Non-Crystalline Solids*, *547*(2020), pp. 120306.

[8] Sen, S., *et al*., Recent Developments in Biomass Derived Cellulose Semi-Transparent Materials for Thermal Insulation Application: A Review, *Cellulose*, *29*(2022), pp. 4805–4833.

[9] Yang, J., *et al.*, Modeling and Coupling Effect Evaluation of Thermal Conductivity of Ternary Opacifier/Fiber/Semi-Transparent Materials Composites for Super-Thermal Insulation, *Materials and Design*, *133*(2017), pp. 224-236.

[10] Qian, G., *et al.*, Enhanced Thermal Conductivity via In Situ Constructed CNT Semi-transparent materials Structure in Composites, *Advanced Materials Interfaces*, *9*(2022), pp. 2102098.

[11] Huang, D., *et al.*, Preparation and Characterization of Silica Semi-Transparent Materials/Polytetrafluoroethylene Composites, *Materials Research Express*, *6*(2019), pp. 115021.

[12] Yang, M., Li, X., Optimum Convergence Parameters of Lattice Boltzmann Method for Predicting Effective Thermal Conductivity. Computer, *Methods Appl. Mech. Eng. 394*(2022), pp. 114891.

[13] Lou, F., *et al.*, Thermal Insulation Performance of Semi-transparent materials Nano-Porous Materials: Characterization and Test Methods, *Gels*, *9*(2023), pp. 220.

[14] Zhu, C.Y., Li, Z.Y., Modeling of the Apparent Solid Thermal Conductivity of Semi-Transparent Materials, *International Journal of Heat And Mass Transfer*, *120*(2018), pp. 724–730.

[15] Liu, H., *et al*., Experiment and Identification of Thermal Conductivity and Extinction Coefficient of Silica Semi-Transparent Materials Composite, *International Journal of Thermal Science*, 121(2017), pp. 192–203.

[16] Kan, A., *et al.*, Simulation and Experimental Study on Thermal Conductivity of Nano-Granule Porous Material Based on Lattice-Boltzmann Method, *Journal of Thermal Science*, *30*(2019), pp. 248–256.

[17] Tao, W., Sparrow, E.M., Ambiguities Related to the Calculation of Radiant Heat Exchange Between a Pair of Surfaces, *Internal Journal of Heat Mass Transfer*, *28*(1985), pp. 1788-1790.

[18] Wang, M., *et al.*, Preparation and Properties of the Multi-Layer Semi-Transparent Materials Thermal Insulation Composites, *Heat and Mass Transfer*, *54*(2018), pp. 2793–2798.

[19] Kang, H. J., Tao, W. Q., Discussion on the Network Method for the Calculating Radiant Interchange within an Enclosure, *Journal of Thermal Science*, *3*(1994), pp. 130–135.

[20] Lou, F., *et al.*, Numerical Study of the Influence of Coupling Interface Emissivity on Semi-transparent materials Metal Thermal Protection Performance, *Gels*, *7*(2021), pp. 250.

[21] Zhang, H., *et al.*, Effect of Radiative Heat Transfer on Determining Thermal Conductivity of Semi-Transparent Materials using Transient Plane Source Method, *Applied Thermal Engineering*, *114*(2017): pp. 337-345.

[22] Zhang, H., *et al.*, Numerical Study of the Influence of Thermal Radiation on Measuring Semi-Transparent Thermal Insulation Material with Hot Wire Method, *International Communications in Heat and Mass Transfer*, *121*(2021): pp. 105120.

[23] Zhang, H., *et al.*, Influence of Participating Radiation on Measuring Thermal Conductivity of Translucent Thermal Insulation Materials with Hot Strip Method, *Journal of Thermal Science*, *31*(2023): pp. 1023-1036.

[24] Lou, F., *et al.*, Thermal Insulation Performance of Aerogel Nano-Porous Materials: Characterization and Test Methods, *Gels*, *9*(2023): pp. 220.

[25] Dai, Y., *et al.*, Study on the Effect of Semi-Transparency on Thermal Insulation Performance of Silica Aerogel Composites, *Case Studies in Thermal Engineering*, *54*(2024): pp. 104010.

[26] Zhang, X., *et al.*, Analysis and Verification on the Effect of Semi-Transparency on the Thermal Insulation Property of Thermal Protection System, *Science Technology and Engineering*, *19*(2019): pp. 362-368. (in Chinese)

Submitted: 10.06.2024
Revised: 15.08.2024
Accepted: 22.08.2024